Article:
Haggar, J.I.H., Cai, Y., Ghataora, S.S. et al. (2020) High modulation bandwidth of semipolar (11–22) InGaN/GaN LEDs with long wavelength emission. ACS Applied Electronic Materials, 2 (8). pp. 2363-2368. ISSN: 2637-6113

https://doi.org/10.1021/acsaelm.0c00399

ACS APPLIED ELECTRONIC MATERIALS

pubs.acs.org/acsaelm

Letter

High Modulation Bandwidth of Semipolar (11−22) InGaN/GaN LEDs with Long Wavelength Emission

Jack IH. Haggar, Yuefei Cai, Suneal S. Ghataora, Richard M. Smith, Jie Bai, and Tao Wang*

Cite This: *ACS Appl. Electron. Mater.* 2020, 2, 2363−2368

Read Online

ACCESS | Metrics & More | Article Recommendations | Supporting Information

ABSTRACT: Visible light communication requires III-nitride LEDs with a high modulation bandwidth but have c-plane limitations. General illumination requires green/yellow III-nitride LEDs with high optical efficiency that are difficult to achieve on c-plane substrates. Micro-LEDs with a low efficiency are used to obtain a high modulation bandwidth. This paper demonstrates a record modulation bandwidth of 540 MHz for our semipolar green LEDs with a broad area. Semipolar yellow and amber LEDs with modulation bandwidths of 350 and 140 MHz, respectively, have also been reported, and are the longest wavelength III-nitride LEDs. These results agree with differential carrier lifetime measurements.

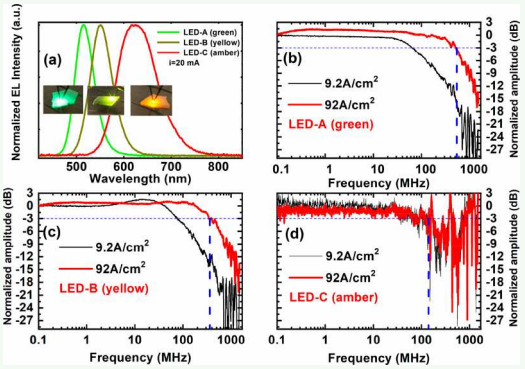

KEYWORDS: *semipolar LEDs, modulation bandwidth, InGaN, recombination lifetime, VLC*

Since the 1990s, there has been unprecedented progress in developing solid-state lighting (SSL) sources, which are overwhelmingly dominated by III-nitride semiconductor light emitting diodes (LEDs). Much like the evolution from traditional telephones to smartphones, it is anticipated that the development of SSL sources will undergo a similar trend from current devices with a single function to future devices with multiple functions. A smart lighting source, for example, can be used as a transmitter for visible light communication (i.e., Li-Fi)[1,2] along with its original function for general illumination.

So far, a "blue LED + yellow phosphor" approach still remains the dominant technique in manufacturing white LEDs, where white lighting is generated by mixing the blue emission of InGaN/GaN LEDs and the downconversion yellow emission from yellow phosphors radiatively pumped by the blue LEDs. However, this approach has a number of fundamental challenges such as limited efficiency, severe color rendering, and instability issues as a result of employing the downconversion phosphors. The even greater concern is due to the phosphors with an intrinsically slow response time on the scale of microseconds, meaning that the resultant bandwidth is limited to be less than 1 MHz.[2−4] Therefore, the ultimate white LED for VLC is possibly a package of either three individual LED chips containing red, green, and blue (i.e., RGB) emissions or at least two LEDs each emitting blue and yellow. High efficiency blue LEDs have been widely commercialized, but one of the remaining challenges is still the optical performance of green and yellow LEDs, the longer emission wavelength emissions, which is far from satisfactory.

In addition to the issues of the downconversion yellow phosphors in current white LEDs for Li-Fi applications, another fundamental issue for Li-Fi applications is due to blue LEDs themselves. Simply speaking, a maximum modulation bandwidth (f) is inversely proportional to the carrier recombination lifetime (τ) of an LED by $f \propto 1/\tau$. Current blue LEDs that are commercially available are grown on c-plane sapphire substrates, intrinsically producing piezoelectric fields as a result of the strain generated by the large lattice mismatch between InGaN and GaN. Consequently, the LEDs exhibit a reduction in the overlap of the electron and hole wave functions leading to an increased radiative recombination lifetime of 10−100 ns, reduced quantum efficiency, and other issues such as efficiency droop.[5,6] Therefore, a maximum attainable modulation bandwidth is in principle on the order of MHz if any extra methods are not used (for example, using micro-LEDs, which will be explained later), which is far from the practical requirements for Li-Fi. In order to enhance the modulation bandwidth when using current blue LEDs for Li-Fi, complicated modulation techniques with pre- and postequalization and a large amount of postprocessing have to be employed, making the communication system

Received: May 14, 2020
Accepted: July 16, 2020
Published: July 16, 2020

https://dx.doi.org/10.1021/acsaelm.0c00399
ACS Appl. Electron. Mater. 2020, 2, 2363−2368

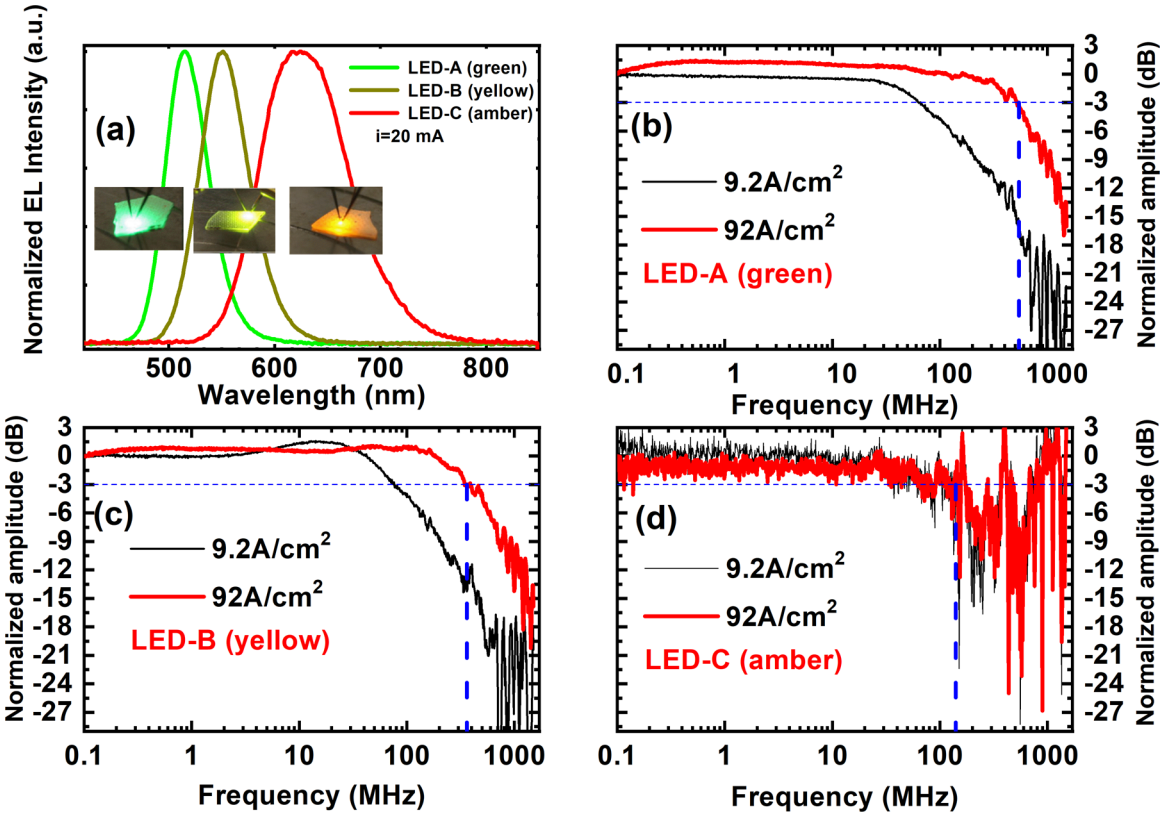

Figure 1. (a) Typical EL spectra of the three LEDs measured at a 20 mA injection current in a CW mode at room temperature. Insets show their respective EL emission images taken at 20 mA, respectively. (b–d) Frequency responses of LED-A (b), and LED-B (c), and LED-C (d).

complicated and expensive.[7−10] Even so, the modulation bandwidth is still far from satisfactory, as it is fundamentally determined by the long radiative recombination lifetime of blue LEDs on c-plane substrates, which is limited by their intrinsic polarization. This increases concerns when LEDs move toward longer emission wavelengths such as green or yellow, which require higher indium content leading to further enhancement in strain-induced piezoelectric fields. Recently, it has been proposed to employ micro-LEDs driven at a very high current density to achieve a high modulation bandwidth for Li-Fi applications.[11−14] However, the great challenge is that the optical efficiency of current micro-LEDs is too low as a result of significantly enhanced nonradiative recombination.[15−17] Therefore, this cannot meet the requirements for both Li-Fi and general illumination simultaneously.

One of the most promising approaches to overcoming the intrinsic polarization is to grow LEDs along a nonpolar or semipolar orientation. In terms of effectively reducing the intrinsic polarization, nonpolar LEDs would be best. However, InGaN intrinsically suffers limited indium incorporation efficiency if it is grown on nonpolar GaN, meaning that it is extremely challenging to grow nonpolar LEDs with green or yellow or any other longer wavelength emissions.[18−22] In contrast, indium atoms can be accommodated on a semipolar GaN surface more easily than those on either a c-plane surface or nonpolar surface,[20] making semipolar GaN more attractive for obtaining longer wavelength LEDs, which require higher indium content. Out of all the semipolar orientations, (11−22) GaN is possibly the best choice when considering all factors including high indium content InGaN,[18−22] a reduction in strain-induced piezoelectric fields, and a short carrier recombination lifetime (by referring to a topical review for the details about III-nitride semipolar LEDs[21]). This makes (11−22) semipolar LEDs strong candidates for achieving longer wavelength LEDs for high speed applications.

It is therefore interesting to explore the upper limit in the maximum modulation bandwidth of semipolar LEDs with green or yellow or any other longer wavelength emissions and beyond for which there are no reports so far. Prior to starting the investigation, the crystal quality of semipolar (11−22) GaN on the more widely used sapphire substrate needs to be improved to a point where it is similar to or at least approaching its c-plane counterpart. In order to meet the material challenges, our group has established a number of cost-effective approaches to achieve high quality semipolar (11−22) GaN grown on m-plane sapphire, leading to the demonstration of high performance semipolar InGaN LEDs covering a wide wavelength range up to amber.[22]

In this work, frequency response measurements have been performed on semipolar (11−22) LEDs with long emission wavelengths from green to amber demonstrating a modulation bandwidth of up to 540 MHz for green LEDs with a typical size of 330 × 330 μm^2, a record modulation bandwidth for III-nitride macro-LEDs (not micro-LEDs) reported so far. This paper also presents the first report on the modulation bandwidth of III-nitride based yellow and amber LEDs and is also the record for the longest wavelength III-nitride LED achieved.

Three different LEDs each containing an InGaN single quantum well (SQW) with different InN mole fractions were prepared on our overgrown semipolar (11−22) GaN with a significantly improved crystal quality on m-plane sapphire by metal−organic chemical vapor deposition (MOCVD). Our detailed structural characterization including both X-ray

https://dx.doi.org/10.1021/acsaelm.0c00399
ACS Appl. Electron. Mater. 2020, 2, 2363−2368

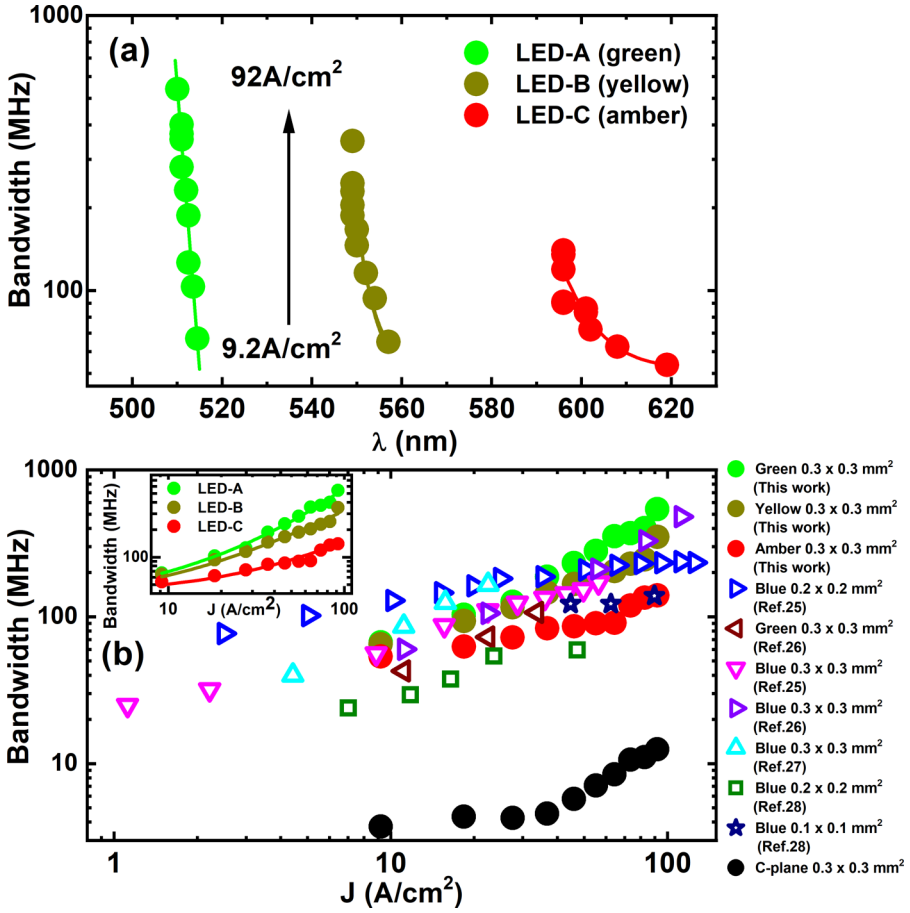

Figure 2. (a) Modulation bandwidth (3 dB) as a function of injection current density from 9.2 to 92 A/cm^2 and the corresponding emission wavelength for each injection current density for the three LEDs. (b) Benchmarking our device performance against current state-of-the-art data from semipolar macro-LEDs (>100 × 100 μm^2) in terms of the 3 dB modulation bandwidth. Our data obtained in this work are exhibited by solid symbols, while data collected from the literature are presented as open symbols with different colors. The inset only includes our data from LED-A, LED-B, and LED-C.

diffraction and transmission electron microscopy measurements confirm that our overgrown semipolar (11−22) GaN templates typically exhibit a dislocation density of 2 × 10^8 /cm^2, which has been achieved using our mature overgrowth approach on regularly arrayed microrod templates.[21−24] The crystal quality is even better than that of standard c-plane GaN on sapphire for the growth of c-plane LEDs. All three LEDs exhibit a similar structure except for in the indium content of their InGaN quantum well. These three LEDs are labeled as LED-A, LED-B, and LED-C, respectively, corresponding to the green LED at 515 nm, the yellow LED at 550 nm, and the amber LED at 610 nm. Please refer to our previous papers for detailed information about the growth of these three LEDs.[22−24] Using a photolithography technique and then a dry-etching process, LEDs with typical dimensions of 330 × 330 μm^2 have been fabricated. A transparent p-contact consisting of a 100 nm thick ITO film was deposited using an electron beam deposition technique and then annealed by rapid thermal annealing (RTA). A Ti/Al/Ti/Au metal stack was then evaporated onto the n-GaN to form an n-contact. Ti/Au was finally prepared on both the p- and n- contacts to form the n- and p-electrode pads.

A standard system has been used to perform modulation bandwidth measurements on these LEDs. To measure the frequency response, a DC bias from a source meter (Keithley 2612B) was added to a bias tee (Tektronix PSPL5575A) along with a small sinusoidal signal with an amplitude of 100 mV from port 1 of a vector network analyzer (VNA, Tektronix TTR506A). The combined signal was sent to our RF probe station equipped with a DC to a 40 GHz signal-ground RF probe (FormFactor ACP40-GS300RC). The electroluminescence (EL) was collected using an infinity corrected objective (10×, NA = 0.28) and then coupled into a multimode fiber using a parabolic collimator (Thorlabs RC12SMA-P01). A photoreceiver (Femto HSA-1G4-Si-FC) consisting of a silicon photodiode with an integrated transimpedance amplifier was used for optical to electrical conversion and the amplified electrical signal was sent to port 2 of the network analyzer. The RF cables and bias tee were also accounted for in the calibration of the S21 transmission. The photoreceiver has a 3 dB modulation bandwidth of 1.4 GHz, and our RF probes are designed for 40 GHz testing, ensuring that the frequency response of our devices is not limited by the system response.

Figure 1a shows the typical electroluminescence (EL) spectra of the three LEDs measured at a 20 mA injection current in a continuous wave (CW) mode at room temperature, demonstrating strong EL emission centered at 515, 550, and 610 nm for LED-A, LED-B, and LED-C, respectively. Insets shows the EL emission images of these three LEDs taken at an injection current of 20 mA.

Figure 1b−d shows the frequency responses of our three LEDs, namely, the normalized output power as a function of

https://dx.doi.org/10.1021/acsaelm.0c00399
ACS Appl. Electron. Mater. 2020, 2, 2363−2368

frequency for the three LEDs measured under identical conditions. The frequency response measurements have also been carried out as a function of injection current density ranging from 9.2 to 92 A/cm^2, which cover the major range for practical applications. As a demonstration, Figure 1b−d only displays the data measured at the lowest and the highest injection current densities for clarity, which are 9.2 and 92 A/cm^2, respectively. The normalized power is obtained by taking the initial frequency point (100 kHz) as 0 dB.

All of the devices demonstrate a maximum 3 dB modulation bandwidth exceeding 100 MHz when driven at a higher current density. For example, LED-A shows a 3 dB modulation bandwidth of 540 MHz at 92 A/cm^2, which is the highest report on III-nitride LEDs with a standard area of 330 × 330 μm^2 or above (not micro-LEDs) for general illumination. LED-B and LED-C exhibit a maximum 3 dB modulation bandwidth of 350 and 140 MHz, both of which are the first report in the yellow and amber regions. The small "shoulder" around 20 MHz apparent on the yellow LED may be due to the relaxation resonant frequency often observed in laser diodes,[25] but in LEDs, this needs further study. Small fluctuations at higher frequencies (before the noise floor of the VNA) are from signal reflections within our testing system. It is worth highlighting that there still exists piezoelectric polarization in semipolar LEDs, although the polarization in semipolar LEDs is substantially weaker compared with that of their c-plane counterparts as stated above. Longer wavelength LEDs require higher indium content, leading to an increase in piezoelectric polarization and thus a reduced quantum efficiency. Consequently, the signal-to-noise ratio (SNR) decreases with increasing emission wavelength. This is why the amber LED signal is noisy compared with other LEDs.

Figure 2a displays the 3 dB modulation bandwidth as a function of injection current density from 9.2 to 92 A/cm^2 for the three LEDs. During the frequency response measurements at each injection current density, the EL spectra of the three LEDs have been measured simultaneously, and Figure 2a also provides their corresponding emission wavelengths. For LED-A, the emission wavelength shows a slight blue-shift with increasing injection current density as a result of the screening effect of polarization-induced electrical fields. LED-B exhibits a slightly enhanced blue-shift in emission wavelength with increasing injection current density compared to LED-A. However, it is worth highlighting that the blue-shift in emission wavelength is much smaller than that of their c-plane counterparts as a result of the intrinsically low polarization of semipolar LEDs. LED-C initially exhibits a large blue-shift in emission wavelength at low injection current densities as a result of band-filling of localized states,[22] and then, the blue-shift reduces quickly but is still larger than those for LED-A and LED-B. It is worth noting that LED-C exhibits amber emission at 596 nm even under 92 A/cm^2 and red emission at 620 nm under 9.2 A/cm^2. Therefore, our LEDs have demonstrated a high frequency response in a wide spectral region, which has not been previously reported. The line width of the semipolar LEDs as a function of injection current can be referred to in the Supporting Information.

Figure 2b benchmarks our device performance against the current state-of-the-art semipolar macro-LEDs (>100 × 100 μm^2) in terms of the 3 dB modulation bandwidth.[26−29] The inset includes only our data from LED-A, LED-B, and LED-C, provided to make them easier to observe. In the current literature, there has been an entire absence of data from longer emission wavelengths such as yellow and amber LEDs, and thus, the majority of devices reported on so far are blue LEDs whose emission wavelength is below 500 nm. One of the major reasons is due to it being extremely challenging to obtain III-nitride based yellow and amber LEDs with reasonably good device performance. Our data obtained in this work are all labeled by solid symbols in Figure 2, while all the data from literature are presented by using open symbols. A conventional c-plane blue LED with a standard size of 330 × 330 μm^2 measured under identical conditions has also been provided as a reference. As expected, the c-plane blue LED (where 2.5 nm InGaN quantum wells are typically used as an active region) exhibits a low 3 dB modulation bandwidth of 4 MHz at a 9.2 A/cm^2 current density and 12.5 MHz at 92 A/cm^2.

The inset in Figure 2b shows that the green LED (i.e., LED-A) exhibits the highest 3 dB bandwidth of 540 MHz at 92 A/cm^2, which is much larger than that of its c-plane blue counterpart. This is followed by the yellow LED at 350 MHz and then the amber LED at 140 MHz, also higher than that of the c-plane blue counterpart, although the indium content in any c-plane blue LED is much lower than those of LED-A−C. This demonstrates the major advantage of semipolar LEDs, which exhibit intrinsically weak polarization. However, it is worth highlighting that the significantly low polarization for semipolar LEDs does not mean that the polarization is zero. Furthermore, with increasing indium content in InGaN, the polarization in semipolar LEDs increases due to the enhancement in strain. Consequently, the carrier recombination lifetime of the semipolar LEDs also increases with increasing emission wavelength (i.e., increasing indium content), although this increase is not so significant as in its c-plane counterparts. As stated earlier, a modulation bandwidth is inversely proportional to the carrier recombination lifetime of a LED. The polarization of an III-nitride LED, which is enhanced with increasing emission wavelength (this requires higher indium content) will lead to a long recombination lifetime. As a result, the modulation bandwidth decreases with increasing emission wavelength. With increasing injection current density, the polarization can be partially screened out, leading to a reduction in carrier recombination lifetime. Of course, if a very high injection current density, beyond what is used in this work is employed (for example, in the case of micro-LEDs, where the emission mechanism is fully dominated by a nonradiative recombination mechanism), the situation is different and thus is beyond the scope of this work.

More interestingly, by fitting the data from LED-A, LED-B, and LED-C, it can be found that the 3 dB modulation bandwidth of these three LEDs as a function of injection current density follows a strong power law relationship, $f_{3dB} \propto J^k$. This suggests that a junction capacitance effect is not a limiting factor in the 3 dB modulation bandwidth of each device when the injection current density is below 92 A/cm^2.[26] This means that a further increase in 3 dB bandwidth can be possibly achieved.

The above small-signal microwave method can also be used to determine a differential carrier lifetime. The detailed expression is given below[30,31]

$$\tau_{\Delta n} = 1/(2\pi f_{3dB}) \quad (1)$$

Where $\tau_{\Delta n}$ is the differential carrier lifetime, and f_{3dB} is the modulation bandwidth.

https://dx.doi.org/10.1021/acsaelm.0c00399
ACS Appl. Electron. Mater. 2020, 2, 2363−2368

Figure 3 exhibits the differential carrier lifetime as a function of injection current density for the three LEDs, demonstrating

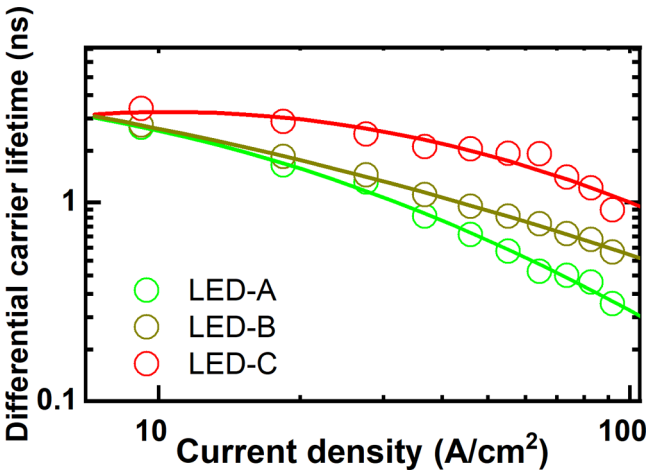

Figure 3. Differential carrier lifetimes of the three LEDs as a function of injection current density, which are extracted from the frequency response measurements. Solid lines are guides to the eye.

that the differential carrier lifetime increases with increasing emission wavelength. Furthermore, in each case, the differential carrier lifetime decreases with increasing injection current density. At 92 A/cm^2, LED-A shows a differential carrier time of 0.31 ns, which is shorter than that of LED-B, whose differential carrier lifetime is 0.56 ns. Both values are consistent with the carrier recombination lifetime with similar emission wavelengths obtained by time-resolved photoluminescence measurements,[32] although a differential carrier lifetime, which also considers transport effects, is different from a carrier recombination lifetime (the former is typically smaller than the latter by a factor of 2−3).[33] Of course, as expected, LED-C (amber LED) exhibits a stronger polarization than LED-A and LED-B. Consequently, LED-C exhibits a differential carrier lifetime of 0.92 ns, which is longer than those for LED-A and LED-B. This result also confirms that a reduction in carrier recombination lifetime with increasing injection current density can be attributed to the screening effect mentioned above. In contrast, the c-plane LED exhibits a typical differential carrier lifetime of >12 ns, which is far longer than those of our semipolar LEDs.

However, it is worth noting that the differential carrier lifetimes of the semipolar LEDs are much shorter than those of any c-plane III-nitride LEDs, although the indium content in these semipolar LEDs is much higher than that for any c-plane blue LEDs. This further confirms that the fundamental physics for the significantly enhanced modulation bandwidth for these semipolar LEDs with long emission wavelengths is due to their intrinsically short recombination lifetime.

In conclusion, we have demonstrated a modulation bandwidth of 540 MHz for semipolar (11−22) green LEDs with typical dimensions of 330 × 330 μm^2, which is a record modulation bandwidth for III-nitride macro-LEDs (not micro-LEDs) reported so far. We also demonstrated a modulation bandwidth of 350 MHz for the semipolar (11−22) yellow LEDs and 140 MHz for the semipolar (11−22) amber LEDs, which are the first report for the longest wavelength III-nitride LEDs with such a high modulation bandwidth. All these long wavelength III-nitride LEDs are grown on our overgrowth semipolar (11−22) GaN with a significantly improved crystal quality on m-plane sapphire. The differential carrier lifetimes of these long wavelength LEDs have been extracted from frequency response measurements, further confirming that the significantly enhanced modulation bandwidth is due to the intrinsically low polarization. This result may pave the way for a next generation white light source, which can meet both the requirements for VLC and general illumination simultaneously.

■ ASSOCIATED CONTENT

Supporting Information

The Supporting Information is available free of charge at https://pubs.acs.org/doi/10.1021/acsaelm.0c00399.

Additional material includes the full width half-maximum of the electroluminescence spectra of all three LEDs as a function of injection current density (PDF)

■ AUTHOR INFORMATION

Corresponding Author

Tao Wang − *Department of Electronic and Electrical Engineering, The University of Sheffield, Sheffield S1 3JD, United Kingdom;* orcid.org/0000-0001-5976-4994; Email: t.wang@sheffield.ac.uk

Authors

Jack IH. Haggar − *Department of Electronic and Electrical Engineering, The University of Sheffield, Sheffield S1 3JD, United Kingdom;* orcid.org/0000-0001-5198-6445

Yuefei Cai − *Department of Electronic and Electrical Engineering, The University of Sheffield, Sheffield S1 3JD, United Kingdom;* orcid.org/0000-0002-2004-0881

Suneal S. Ghataora − *Department of Electronic and Electrical Engineering, The University of Sheffield, Sheffield S1 3JD, United Kingdom*

Richard M. Smith − *Department of Electronic and Electrical Engineering, The University of Sheffield, Sheffield S1 3JD, United Kingdom*

Jie Bai − *Department of Electronic and Electrical Engineering, The University of Sheffield, Sheffield S1 3JD, United Kingdom;* orcid.org/0000-0002-6953-4698

Complete contact information is available at: https://pubs.acs.org/10.1021/acsaelm.0c00399

Author Contributions

T.W. conceived the idea and organized the project. J.H. performed frequency response and EL measurements. J.B. fabricated the device. Y.C. contributed to device testing and involved relevant discussion. S.G. and R.S. contributed to discussion. T.W. and J.H. prepared the manuscript.

Notes

The authors declare no competing financial interest.

■ ACKNOWLEDGMENTS

Financial support is acknowledged from the Engineering and Physical Sciences Research Council (EPSRC), U.K., via EP/P006973/1, EP/P006361/1, and EP/M015181/1

■ REFERENCES

(1) Haas, H. Li-Fi is a paradigm-shifting 5G technology. *Rev. Phys.* **2018**, *3*, 26.

(2) Wang, S. W.; Chen, F.; Liang, L.; He, S.; Wang, Y.; Chen, X.; Lu, W. A high-performance blue filter for a white-led-based visible light communication system. *IEEE Wirel. Commun.* **2015**, *22*, 61.
(3) Chow, C. W.; Yeh, C. H.; Liu, Y. F.; Huang, P. Y.; Liu, Y. Adaptive scheme for maintaining the performance of the in-home white-LED visible light wireless communications using OFDM. *Opt. Commun.* **2013**, *292*, 49.
(4) Le Minh, H.; O'Brien, D.; Faulkner, G.; Zeng, L.; Lee, K.; Jung, D.; Oh, Y.; Won, E. T. 100-Mb/s NRZ visible light communications using a postequalized white LED. *IEEE Photonics Technol. Lett.* **2009**, *21*, 1063.
(5) Bernardini, F.; Fiorentini, V.; Vanderbilt, D. Spontaneous polarization and piezoelectric constants of III-V nitrides. *Phys. Rev. B: Condens. Matter Mater. Phys.* **1997**, *56*, R10024.
(6) Takeuchi, T.; Amano, H.; Akasaki, I. Theoretical study of orientation dependence of piezoelectric effects in wurtzite strained GaInN/GaN heterostructures and quantum wells. *Jpn. J. Appl. Phys.* **2000**, *39*, 413.
(7) Sufyan Islim, M.; Ferreira, R. X.; He, X.; Xie, E.; Videv, S.; Viola, S.; Watson, S.; Bamiedakis, N.; Penty, R. V.; White, I. H.; Kelly, A. E.; Gu, E.; Haas, H.; Dawson, M. D. Towards 10 Gb/s orthogonal frequency division multiplexing-based visible light communication using a GaN violet micro-LED. *Photonics Res.* **2017**, *5*, A35.
(8) Rajbhandari, S.; Jalajakumari, A. V. N.; Chun, H.; Faulkner, G.; Cameron, K.; Henderson, R.; Tsonev, D.; Haas, H.; Xie, E.; Mckendry, J. J. D.; Herrnsdorf, J.; Ferreira, R.; Gu, E.; Dawson, M. D.; O'brien, D. A multigigabit per second integrated multiple-input multiple-output VLC demonstrator. *J. Lightwave Technol.* **2017**, *35*, 4358.
(9) Manousiadis, P.; Chun, H.; Rajbhandari, S.; Mulyawan, R.; Vithanage, D. A.; Faulkner, G.; Tsonev, D.; McKendry, J. J. D.; Ijaz, M.; Enyuan Xie; Gu, E.; Dawson, M. D.; Haas, H.; Turnbull, G. A.; Samuel, I. D. W.; O'Brien, D. Demonstration of 2.3 Gb/s RGB white-light VLC using polymer based colour-converters and GaN micro-LEDs. *2015 IEEE Summer Topicals Meeting Series (SUM 2015)* **2015**, 222−223.
(10) Tsonev, D.; Chun, H.; Rajbhandari, S.; Mckendry, J. J. D.; Videv, S.; Gu, E.; Haji, M.; Watson, S.; Kelly, A. E.; Faulkner, G.; Dawson, M. D.; Haas, H.; O'brien, D. A 3-Gb/s single-LED OFDM-based wireless VLC link using a gallium nitride MLED. *IEEE Photonics Technol. Lett.* **2014**, *26*, 637.
(11) Ji, R.; Wang, S.; Liu, Q.; Lu, W. High-speed visible light communications: enabling technologies and state of the art. *Appl. Sci.* **2018**, *8*, 589.
(12) Jukaria, M.; Singh, B. K.; Kumar, A. Review of Li Fi technology: scope of next generation communication system for home area network. *Int. J. Eng. Sci.* **2018**, *7*, 265.
(13) Mei, S.; Liu, X.; Zhang, W.; Liu, R.; Zheng, L.; Guo, R.; Tian, P. High-bandwidth white-light system combining a micro-LED with perovskite quantum dots for visible light communication. *ACS Appl. Mater. Interfaces* **2018**, *10*, 5641.
(14) Liu, X.; Lin, R.; Chen, H.; Zhang, S.; Qian, Z.; Zhou, G.; Chen, X.; Zhou, X.; Zheng, L.; Liu, R.; Tian, P. High-bandwidth InGaN self-powered detector arrays toward MIMO visible light communication based on micro-LED arrays. *ACS Photonics* **2019**, *6*, 3186.
(15) Olivier, F.; Tirano, S.; Dupré, L.; Aventurier, B.; Largeron, C.; Templier, F. Influence of size-reduction on the performances of GaN-based micro-LEDs for display application. *J. Lumin.* **2017**, *191*, 112.
(16) Konoplev, S. S.; Bulashevich, K. A.; Karpov, S. Y. From large-size to micro-LEDs: scaling trends revealed by modeling. *Phys. Status Solidi A* **2018**, *215*, 1700508.
(17) Bai, J.; Cai, Y.; Feng, P.; Fletcher, P.; Zhao, X.; Zhu, C.; Wang, T. A direct epitaxial approach to achieving ultra-small and ultra-bright InGaN-based micro light emitting diodes (μLEDs). *ACS Photonics* **2020**, *7*, 411−415.
(18) Masui, H.; Nakamura, S.; DenBaars, S. P.; Mishra, U. K. Nonpolar and semipolar III-nitride light-emitting diodes: achievements and challenges. *IEEE Trans. Electron Devices* **2010**, *57*, 88.
(19) Strittmatter, A.; Northrup, J. E.; Johnson, N. M.; Kisin, M. V.; Spiberg, P.; El-Ghoroury, H.; Usikov, A.; Syrkin, A. Semi-polar nitride surfaces and heterostructures. *Phys. Status Solidi B* **2011**, *248*, 561.
(20) Northrup, J. E. GaN and InGaN (11−22) surfaces: Group-III adlayers and indium incorporation. *Appl. Phys. Lett.* **2009**, *95*, 133107.
(21) Wang, T. Topical review: development of overgrown semi-polar GaN for high efficiency green/yellow emission. *Semicond. Sci. Technol.* **2016**, *31*, 093003.
(22) Bai, J.; Xu, B.; Guzman, F. G.; Xing, K.; Gong, Y.; Hou, Y.; Wang, T. 11−22) semipolar InGaN emitters from green to amber on overgrown GaN on micro-rod templates. *Appl. Phys. Lett.* **2015**, *107*, 261103.
(23) Zhang, Y.; Bai, J.; Hou, Y.; Yu, X.; Gong, Y.; Smith, R. M.; Wang, T. Microstructure investigation of semi-polar (11−22) GaN overgrown on differently designed micro-rod array templates. *Appl. Phys. Lett.* **2016**, *109*, 241906.
(24) Gong, Y.; Xing, K.; Xu, B.; Yu, X.; Li, Z.; Bai, J.; Wang, T. High efficiency green-yellow emission from InGaN/GaN quantum well structures grown on overgrown semi-polar (11−22) GaN on regularly arrayed micro-rod templates. *ECS Trans.* **2015**, *66*, 151.
(25) Lee, C.; Zhang, C.; Becerra, D. L.; Lee, S.; Forman, C. A.; Oh, S. H.; Farrell, R. M.; Speck, J. S.; Nakamura, S.; Bowers, J. E.; Denbaars, S. P. Dynamic characteristics of 410 nm semipolar (20−21) III-nitride laser diodes with a modulation bandwidth of over 5 GHz. *Appl. Phys. Lett.* **2016**, *109*, 101104.
(26) Dinh, D. V.; Quan, Z.; Roycroft, B.; Parbrook, P. J.; Corbett, B. GHz Bandwidth semipolar (112−2) InGaN/GaN light-emitting diodes. *Opt. Lett.* **2016**, *41*, 5752.
(27) Corbett, B.; Quan, Z.; Dinh, D. V.; Kozlowski, G.; O'Mahony, D.; Akhter, M.; Schulz, S.; Parbrook, P.; Maaskant, P.; Caliebe, M.; Hocker, M.; Thonke, K.; Scholz, F.; Pristovsek, M.; Han, Y.; Humphreys, C. J.; Brunner, F.; Weyers, M.; Meyer, T. M.; Lymperakis, L. Development of semipolar (11−22) LEDs on GaN templates. *Proc. SPIE* **2016**, *9768*, 97681G.
(28) Quan, Z.; Dinh, D. V.; Presa, S.; Roycroft, B.; Foley, A.; Akhter, M.; O'mahony, D.; Maaskant, P. P.; Caliebe, M.; Scholz, F.; Parbrook, P. J.; Corbett, B. High bandwidth freestanding semipolar (11−22) InGaN/GaN light-emitting diodes. *IEEE Photonics J.* **2016**, *8*, 1.
(29) Haemmer, M.; Roycroft, B.; Akhter, M.; Dinh, D. V.; Quan, Z.; Zhao, J.; Parbrook, P. J.; Corbett, B. Size-dependent bandwidth of semipolar (11−22) light-emitting-diodes. *IEEE Photonics Technol. Lett.* **2018**, *30*, 439.
(30) Rajabi, K.; Wang, J.; Jin, J.; Xing, Y.; Wang, L.; Han, Y.; Sun, C.; Hao, Z.; Luo, Y.; Qian, K.; Chen, C.-J.; Wu, M.-C. Improving modulation bandwidth of c-plane GaN-based light-emitting diodes by an ultra-thin quantum wells design. *Opt. Express* **2018**, *26*, 24985.
(31) Monavarian, M.; Rashidi, A.; Aragon, A. A.; Oh, S. H.; Rishinaramangalam, A. K.; DenBaars, S. P.; Feezell, D. Impact of crystal orientation on the modulation bandwidth of InGaN/GaN light-emitting diodes. *Appl. Phys. Lett.* **2018**, *112*, 041104.
(32) Liu, B.; Smith, R.; Athanasiou, M.; Yu, X.; Bai, J.; Wang, T. Temporally and spatially resolved photoluminescence investigation of (11−22) semi-polar InGaN/GaN multiple quantum wells grown on nanorod templates. *Appl. Phys. Lett.* **2014**, *105*, 261103.
(33) Coldren, L. A.; Corzine, S. W.; Mašanović, M. L. *Diode Lasers and Photonic Integrated Circuits*, 2nd ed.; John Wiley & Sons, 2012; p 257.

https://dx.doi.org/10.1021/acsaelm.0c00399
ACS Appl. Electron. Mater. 2020, 2, 2363−2368